Proceedings of the 8th World Congress on Momentum, Heat and Mass Transfer (MHMT'23)
Lisbon, Portugal – March 26 – 28, 2023
Paper No. ICMFHT 109
DOI: *10.11159/icmfht23.109*

Airlift Pumps with Annulus Risers: An Experimental Investigation

Shahriyar G. Holagh[1*], Dana Fadlalla[1], Marwan H. Taha[1], Alexander Doucette[1], Wael H. Ahmed[1]
School of Engineering, University of Guelph,
Guelph, N1G 2W1, ON, Canada
*Ghazanfs@uoguelph.ca

Abstract **–** Airlift pumps are used in many industries. In these pumps, the performance is strongly affected by the geometrical design conditions. In this study, the performance of an airlift pump is experimentally evaluated for both circular and annulus pump risers. An airlift pump operating under air-water two-phase flow conditions was tested using a dual pump injector and for a constant submergence ratio. Capacitance sensors are used to measure the instantaneous void fraction through the pump riser, while high-speed images are analyzed to identify the interfacial structures of the air-water two-phase flow patterns through the pump risers. The results show that the water flow rate and efficiency of the pump for both risers are strongly dependent on the flow-pattern. In the annulus riser, higher liquid flow rates and pump efficiency are achieved at low gas flow rates, where slug pattern exists, while for the circular riser, the pump performs better at higher gas flow rates. Also, void fraction was found to be higher in the annulus riser for the entire range of gas flow rate due to the smaller cross-sectional area and the faster gas phase velocity through this area. Moreover, in the annulus riser, the Taylor bubble exhibited rotational motion around the pipe axis while moving upward. The length of Taylor bubbles in the pump riser was found to be longer and move with higher velocity and frequency in the case of the annulus riser, which is contributing to the better pump performance at low air flow rates.

Keywords**:** Airlift Pump; Annulus Riser; Performance; Efficiency; Void Fraction; Air-water

1. Introduction

Airlift pumps are usually utilized for flow recirculation and aeration purposes in many industrial applications like aquaculture and sewage treatment, while they can be used to lift heavy and viscous liquids/mixtures such as hydrocarbons in oil and gas extraction or moving explosive and toxic liquids in chemical processing plants. An airlift pump is composed of a vertical pipe (i.e., riser) submerged into liquid tank and connected to a gas injector at the bottom, where gas is injected and leads to the creation of a gas-liquid mixture within the riser. The two-phase mixture has lower specific gravity; this, in turn, pushes the liquid phase upward, and pumping is accomplished. Having no moving mechanical components, these pumps offer low maintenance costs and more reliable operation while consuming less energy compared to conventional rotary pumps [1].

Literature review shows that both the lifted liquid flow rate vs. injected gas flow rate and efficiency (the ratio of the work used for lifting liquid to the work entering the system through isothermal expansion of the gas phase) curves of airlift pumps are influenced by operating and geometrical design conditions. Two-phase flow pattern within the riser, injected gas flow rate, void fraction, and working fluids are the most important operating conditions affecting their performance. On the other hand, geometrical aspects like submergence ratio (submerged length divided by the total riser length), riser diameter and length, injector design conditions (gas injection method and location) also strongly impact the pumps performance. Several studies have investigated altering the operating and geometrical conditions to improve the pump performance both experimentally and numerically. Generally, four common types of two-phase flow pattern (bubbly, stable and unstable slug, churn, and annular) have been observed in airlift pumps (Kassab et al. [2], [3], Hanifzadeh et al. [4], Ligus et al. [5], Charalampos et al. [6]). According to the literature, the pump performance is flow pattern dependent. That is, depending on the geometrical design, bubbly-slug transition [7], slug flow pattern [2] or slug-churn transition [8], [9] has been observed to give the highest efficiency, while slug-churn/churn flow patterns have been seen to result in the highest performance (i.e., increased liquid flow rate) [4]. Majority of the conducted studies have concentrated on the impact of operating and geometrical parameters on airlift pumps performance. According to the literature, the performance curve of airlift pumps is a function gas flow rate and pressure as well as submergence ratio and riser length and diameter [2], [10], [11]. In fact, lifted

liquid flow rate increases with increasing injected gas flow rate and reaches a maximum value (slug-churn transition), is followed by a slight decrease and then, remains nearly unchanged (churn and annular regimes) [2], [12], [13]. However, with increasing gas flow rate, the pump efficiency increases first to a maximum point and then, drastically declines [2]. The study conducted by Kassab et al. [2] showed that maximum efficiency does not necessarily takes place at the maximum liquid flow rate.

Larger submergence ratios contribute to a better performance, i.e., increased liquid flow rate, due to the higher static pressure of the liquid column in the riser [2], [3], [11], [13–17]. Also, increasing submergence ratio has been found to reduce the minimum gas flow rate needed to lift the liquid phase [2], [12]. Also, Kassab et al. [2] found that increasing riser length (static lift) at constant submergence ratio can lead to slight improvement in the pump performance. Another important geometrical parameter is the riser diameter. Fan et al. [18] and Qiang et al. [15] found that upwelling efficiency of airlift pumps increases with the increase of riser diameter (from 0.4 m to 2.0 m) due to lower friction in larger pipes. The same increasing effect on performance for small diameter risers, 3-25 mm and 12-19 mm, had been seen by Reinemann et al. [19] and Kouremenos and Staicos [20]. However, the findings of Kim et al. [21] revealed that as the riser diameter increases, the pump performance declines (i.e., lower liquid flow rates are resulted) and the minimum gas flow rate for lifting liquid increases. Dare et al. [22] also reached the same conclusion; they discovered that small diameter risers deliver a higher lift.

Majority of airlift pumps' performance studies have investigated them under wide ranges of operating and geometrical conditions for risers with circular cross-section. However, in the case where annulus pump riser is required for either operational purposes or to gain access to the core of pump risers such as in nuclear applications, no available data was found in the literature. To the best knowledge of the authors, only one study (Sohn et al. [23]) has studied the effect of inserting a blunt body into the riser of an airlift pump on its performance. They discovered that blunt body-inserted riser and circular riser exhibit different behaviors in terms of bubbles rising velocity and wall friction despite having the same flow area; this was attributed to the inevitable difference in the hydraulic diameters and wall areas between the two risers. It was also found that at different submergence ratios, the blunt body-inserted riser delivers higher pumping performance (i.e., higher liquid flow rates) at low inlet gas flow rates because of lower bubble rising velocities, whilst at high gas flow rates, the circular riser gives higher performance since it has lower frictional losses. However, this study failed to compare flow patterns and the characteristics of the bubbles between the two riser configurations. Moreover, they investigated pump's performance at a limited inlet gas flow rate range; that is, the study did not cover high gas flow rates where performance curve passes its maximum point. Furthermore, void fraction data and associated characteristics were not discussed. To fill above-mentioned gaps, this study compares the performance of an airlift pump for annulus and circular risers under a wide range of inlet gas flow rate. Also, flow patterns and large bubbles characteristics (length, velocity, and frequency of appearance as well as their shape and movement dynamics) together with void fraction data are compared between the two geometrical configurations. The study has been conducted experimentally; all experiments have been carried out at one submergence ratio of 0.7 (i.e., Sr=70%) using a dual air injector.

2. Methodology

2.1. Experimental apparatus

Test loop used in this study is the one used by Abed et al. [24] (see Fig. 1). Fig. 1 is a schematic of the experimental configuration using an airlift pump. To keep the liquid level in the secondary supply tank constant so that the submergence ratio of the airlift pump system could be calculated, liquid from a reservoir tank was pumped into it. The static head, Hs, is divided by the pipe's overall length, L, to determine the submergence ratio. The submergence ratio for the collection of air-liquid experiments was set to 70%. To form a two-phase mixture and pump the liquid up the riser, air was added to the liquid using the gas lift pump. Mass flow controllers (MFC) were used to regulate the air flow rate throughout a range of 4 liters per minute (LPM) to 60 LPM, which were the minimum and maximum air flow respectively. The setup's collection tank, located on top, channeled fluids toward a measurement tank with one-liter intervals, which was used to gauge the volume of collected liquid. The volumetric liquid flow rate (LPM) was determined by timing the flow of water collected in the measurement tank using a human-operated stopwatch. In addition, two-phase flow patterns, bubble length, and bubble velocity along the airlift riser pipe were examined using high-speed imaging. Instantaneous void fraction data was collected using a capacitance sensor. Fig. 2 indicates a schematic drawing of the air injector and Fig. 3 shows the dimensions of the annulus used; both circular and annulus risers have the same

diameter of OD = $1\,{}^{1}/_{4}{}''$ and length of 1.57 m. The uncertainty analysis of the measured parameters is provided in Table 1.

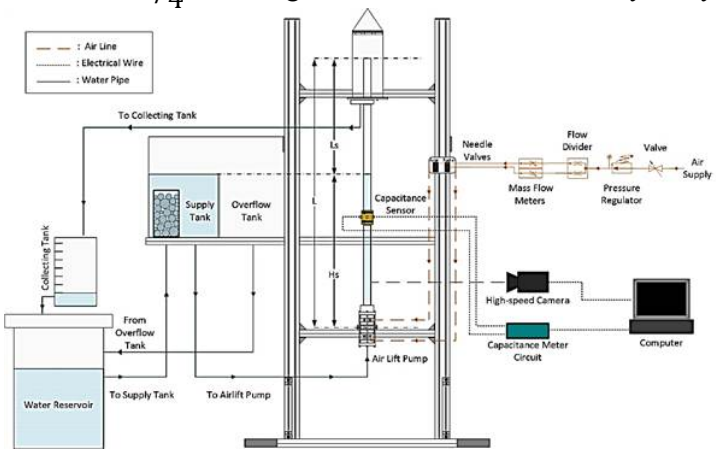

Fig. 1: Schematic diagram of the test loop. Redrawn and modified with permission from Abed et al. [24]. Copyright 2022 Elsevier.

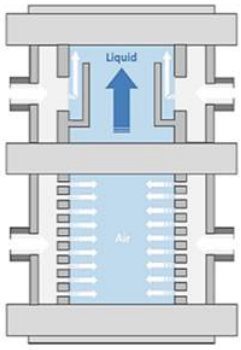

Fig. 2: Schematic view of the used airlift. Redrawn and modified with permission from Abed et al. [24]. Copyright 2022 Elsevier.

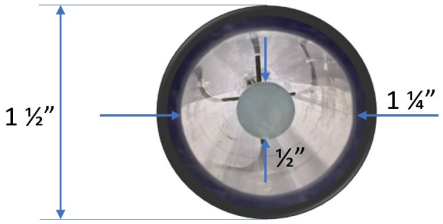

Fig. 3: Annulus riser used

Table 1: Uncertainty analysis

Parameter	Uncertainty
Air mass flow rate	±1.2%
Water mass flow rate	±3.0%
Void fraction	±6.0%
Pump efficiency	±0.3%

2.2. Image processing

High speed images, taken at a location Z/D = 30 downstream of the pump's injector for eight different gas injection rates ranging from 3LPM to 60LPM, were analyzed. The measurement of the bubble velocity was obtained by comparing a set of images that tracked the bubbles displacement between two frames, scaled using the known diameter of the riser, as well as the time elapsed between the frames. Similarly, the bubble length was measured according to the scaled riser diameter. At high flow rates, elongated bubbles were longer than the image frame, thus, the velocity of the bubble was multiplied by the time elapsed between the entry and exit of the bubble to determine the bubble displacement, which also corresponded to the bubble length. Finally, the bubble frequency was obtained by counting the number of passing bubbles with respect to the time elapsed at each flow rate.

3. Results and discussions

3.1. Pumping performance

Figs. 4a and 4b show the lifted liquid flow rate and efficiency for both circular and annulus risers, respectively. Note that the pumping efficiency of the airlift pump has been calculated using the modified version of Nicklin equation that considers the dual injection method [12], as follows:

$$\eta = \frac{\rho g Q_L (L - H_s)}{P_{atm} Q_{Gr} \ln\left(\frac{P_r}{P_{atm}}\right) + P_{atm} Q_{Ga} \ln\left(\frac{P_a}{P_{atm}}\right)} \tag{1}$$

Looking at these figures, one can see that both risers show the same behavior for lifted liquid flow rate and efficiency variations against inlet gas flow rate. That is, in both risers, lifted liquid flow rates drastically increase with increasing gas flow rate and reach their maximum and then, moderately decline. On the other hand, their pumping efficiencies sharply increase up to the maximum points, followed by drastic reductions. At the lowest inlet gas flow rate (0.33 kg/hr), both risers

fail to lift the liquid phase effectively; this is because at this flow rate, flow pattern observed within both risers is slug flow with short Taylor bubbles (see Fig. 10a). The buoyancy of the short Taylor bubbles are not enough to dominate the gravitational forces; therefore, liquid phase is not lifted sufficiently to exit from the risers. As the inlet gas flow rate increases, Taylor bubbles length becomes longer (see Fig. 10a) and the buoyancy force overcomes the gravitational forces; therefore, both lifted liquid flow rate and efficiency increase for each riser. Taylor bubbles act like a piston pushing the liquid phase entrained within the liquid slug upward while moving up. Further increase in gas flow rate leads to transition from slug to churn flow pattern. Long bubbles in churn pattern are longer than Taylor ones and move faster (see Figs. 10a and 10b); also, liquid film surrounding long bubbles in churn pattern do not move downward as opposed to slug flow pattern. As a result, lifted liquid flow rate continues to increase in both risers after the slug-churn transition and reaches a maximum point and then, decreases as the two-phase flow becomes closer to annular flow regime. However, the pumping efficiency of both risers reaches its maximum and drastically declines after the transition point; this is because, long bubbles in churn pattern have lower ability to use the work entered the system through gas phase's isothermal expansion for lifting the liquid phase compared with Taylor bubbles.

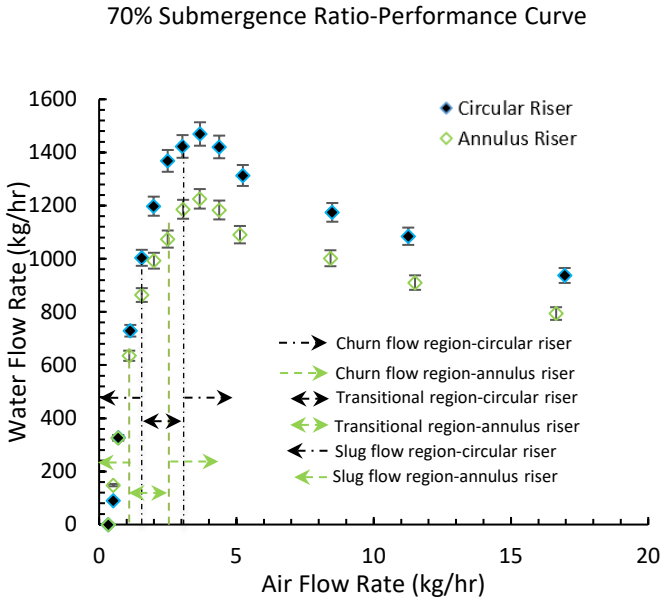

Fig. 4a: Pumping performance of the airlift pump for circular and annulus riser

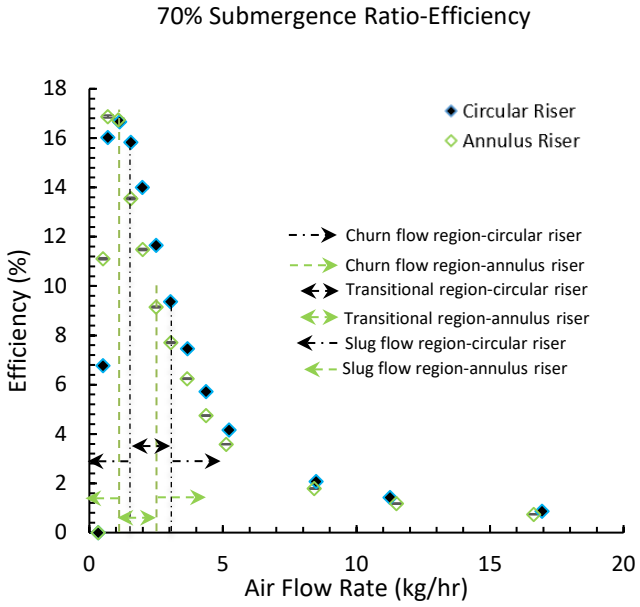

Fig. 4b: Pumping efficiency of the airlift pump for circular and annulus riser

Comparing performance curves between circular and annulus risers (Fig. 4a), one can see that at low inlet gas flow rates (lower than 0.69 kg/hr), the annulus riser delivers more liquid than the circular riser; however, at higher inlet gas flow rates, the circular riser performs better and gives higher liquid flow rates. Also, as the gas flow rate increases, the difference between the lifted liquid flow rates becomes bigger up to the maximum performance point. This is because higher gas flow rates that bring about higher liquid flow rates, the frictional losses within the annulus riser become higher than the circular riser due to larger wall areas; therefore, circular risers perform better at higher gas flow rates. Both circular and annulus risers reach maximum performance in churn flow regime at the same inlet gas flow rate (3.67 kg/hr); however, at maximum performance point, the circular riser delivers nearly 1470 kg/hr of water, whereas the annulus delivers almost 1225 kg/hr of water. That is, maximum water flow rate of the annulus riser is around 16.6% lower than that of the circular riser. After the maximum performance point, the difference between the water flow rates delivered by the risers becomes slightly smaller.

The same behavior is observed in the efficiency curves (Fig. 4b); annulus riser gives higher efficiencies (up to maximum efficiency points) at lower gas flow rates (lower than 0.69 kg/hr) because of its higher liquid flow rate in this region. At higher gas flow rates, this is the circular riser that gives slightly better efficiencies since it delivers more water. However, the difference between the risers' efficiencies becomes smaller and smaller as gas flow rate increases so that they reach nearly the same values at the highest gas flow rate. Both circular and annulus risers reach maximum efficiency in slug flow regime; interestingly, they give almost the same values of maximum efficiency (around 16.7%). However, the circular riser reaches

the maximum efficiency point at a higher gas flow rate than the annulus riser. This is because slug-churn transition takes place at higher gas flow rates in the circular riser compared to the annulus riser. The differences between the circular and annulus risers in terms of performance can be better understood by comparing two-phase flow structures behavior within the riser as described in the following sections.

3.2. Flow patterns

Experimental observations revealed the presence of two two-phase flow patterns including slug and churn flow within both risers under the studied test conditions. Flow patterns were identified by both flow visualization and instantaneous void fraction measurements, both at Z/D=30, where two-phase flow within the riser reaches quasi-developed region [12]. The PDF diagrams of the measured void fraction data have been shown in Figs. 5. Figs. 6 and 7, respectively, reveal the time-series void fraction data and their average values measured in the circular (dashed graphs in Fig. 6) and annulus (continuous graphs in Fig. 6) risers for all 14 test points.

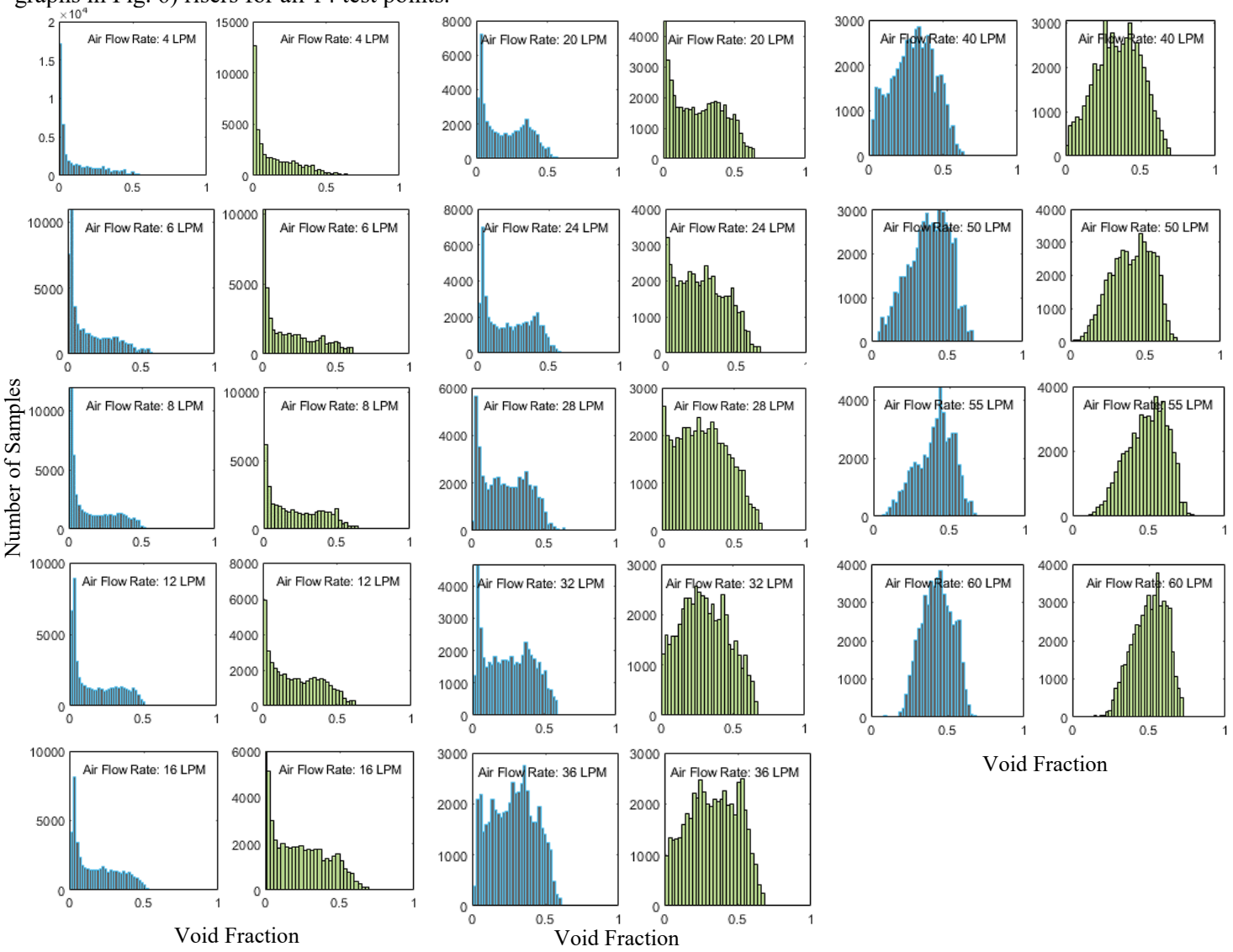

Fig. 5: Void fraction PDFs at Z/D=30 and different inlet gas flow rates for circular (blue bars) and annulus (green bars) risers

According to Figs. 6 and 7, with increasing inlet gas flow rate, instantaneous and subsequently, time-average void fraction increases in both risers; however, the annulus riser gives higher values of void fraction, notably at higher inlet gas flow rates. This is because the annulus riser has smaller cross-sectional area (i.e., smaller hydraulic diameter); this, in turn, allows the gas phase to occupy more area in the annulus riser compared to the circular riser under the same inlet gas flow rates.

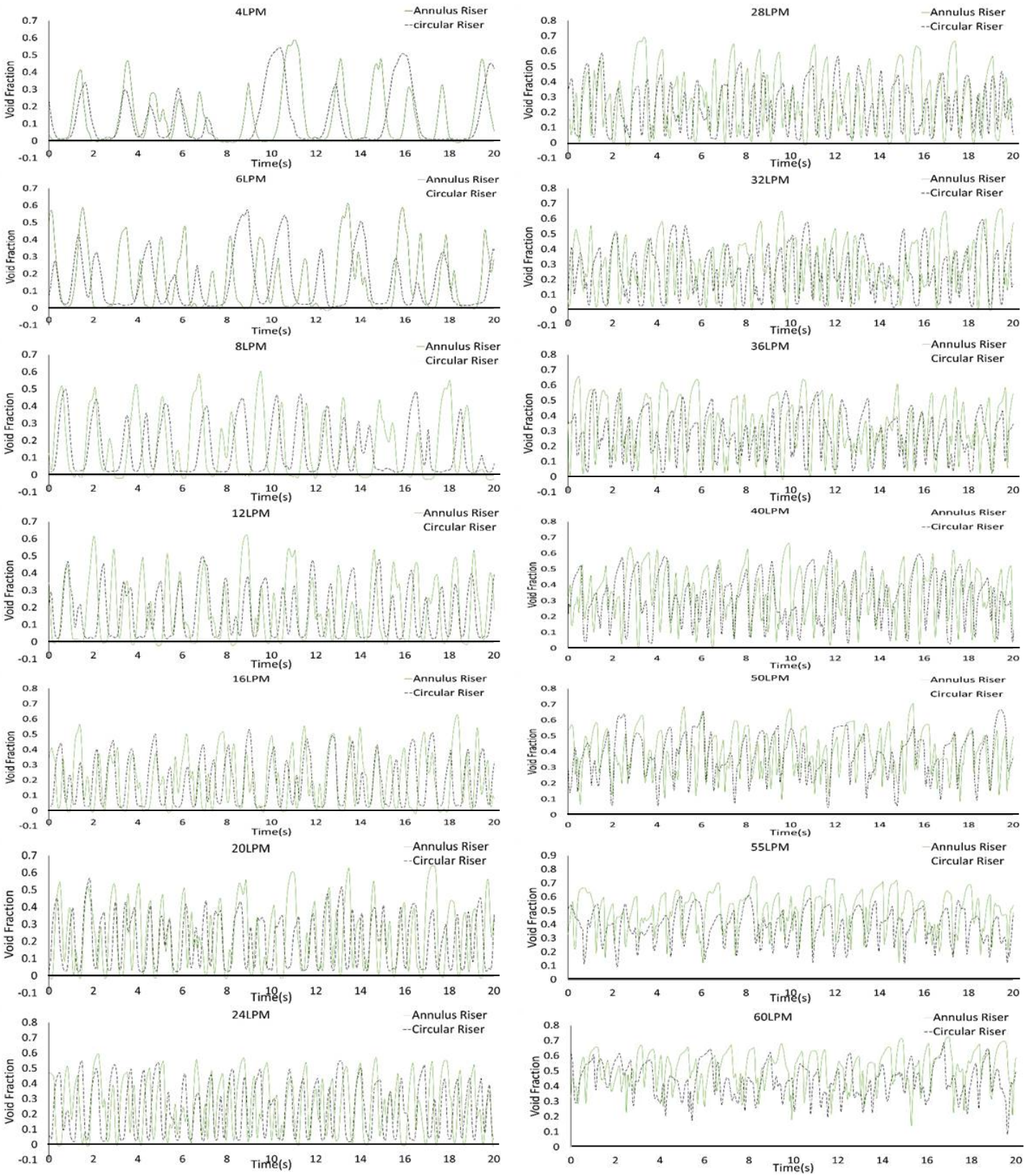

Fig. 6: Time series void fraction results at Z/D=30 and different inlet gas flow rates for circular and annulus risers

Higher void fractions in the annulus riser contribute to faster transition to churn flow. Experimental observations and PDF diagrams comparison show that in the annulus and circular risers, slug flow exists up to inlet gas flow rates of respectively 12 and 16 LPM (average void fraction of almost 19% in both risers), where the PDFs are still showing two peaks. Correspondingly, slug-churn transition starts at 12 and 16 LPM of gas flow rate for these risers and extend to the inlet gas flow rates of 24 LPM and 28 LPM (average void fraction of almost 24% in both risers), respectively, where churn flow appears, and the PDFs become wider and show only one peak. Also, PDF diagrams show that in all slug, slug-to-churn, and churn flow patterns, the annulus riser covers slightly wider ranges of void fraction than the circular riser, leading to wider PDF diagrams in this riser. These differences in void fraction data between the risers can be justified by interfacial structures behavior within the risers as expounded in the next sections.

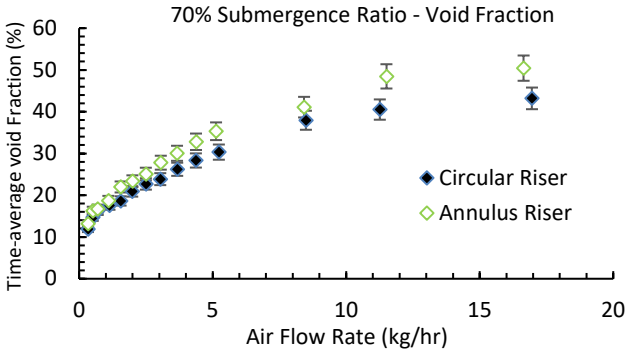

Fig. 7: Time-average void fraction for the risers

3.3. Interfacial structures behavior

Figs. 8 and 9 indicate successive images of slug and churn flow patterns observed in the circular and annulus risers at imaging location of Z/D=30 and inlet gas flow rates of 6 LPM (slug flow) and 24 LPM (churn flow), respectively. As can be seen in the annulus riser, both Taylor bubbles and long bubbles in churn pattern fail to embrace the rod in the middle; this leads to the presence of a narrow path for liquid phase in the body of the large bubbles. Upward flow of the liquid phase through this path imposes drag forces on the large bubbles; this leads Taylor bubbles and long bubbles in churn pattern to have clockwise and counterclockwise rotational movements around the inner rod while moving up as clearly shown in Figs. 8b and 9b, respectively. The rotational movement of the long bubbles is expected to cause a rotational movement in the liquid phase within the liquid slugs above and behind the large bubbles. This is clearly observable by the rotational movement of small bubbles in slug flow pattern and wider dispersion of the aerated region in the liquid slug that occupies almost whole pipe diameter in the annulus riser. Another clear difference is the population and size distribution of small bubbles; as can be seen, in both slug and churn flow patterns, small bubbles are of larger population with smaller diameters in the circular riser. This is because the rotational movement of both large bubbles and liquid slugs in the annulus riser cause more collisions between small bubbles, leading to their coalescence with either themselves or large bubbles at a higher rate.

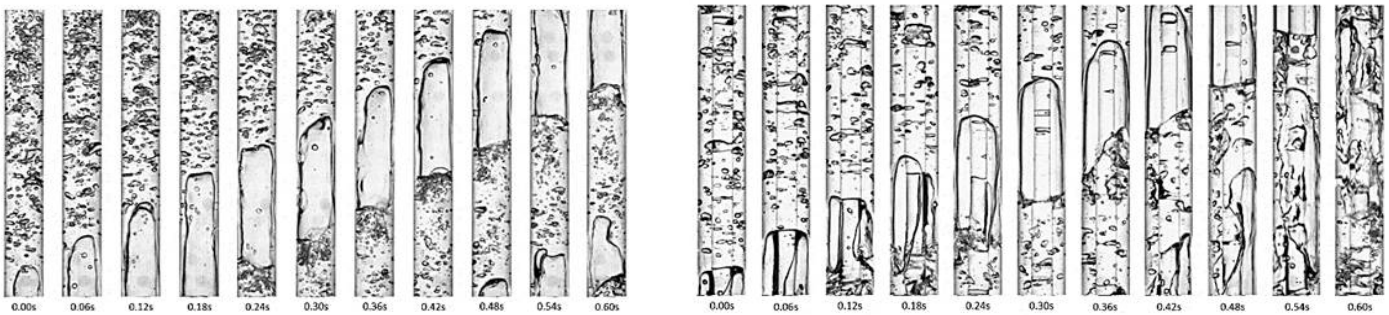

(a) (b)

Fig. 8: Successive images of slug flow pattern observed in (a) circular riser and (b) annulus riser

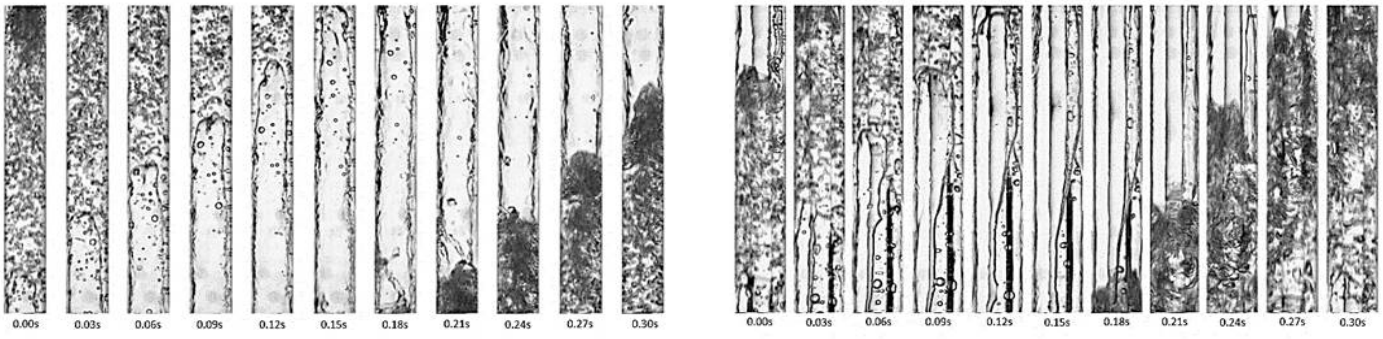

(a) (b)

Fig. 9: Successive images of churn flow pattern observed in (a) circular riser and (b) annulus riser

Figs. 10a, 10b, and 10c respectively represent large bubbles (Taylor bubbles and long bubbles in churn pattern) length, velocity, and frequency of appearance against variations in inlet gas flow rate in both risers. According to these figures, in both risers, large bubbles' length, velocity, and frequency of appearance increase with increasing injected gas flow rate. This is because larger inlet gas flow rates imply larger volume of the gas phase introduced to the riser; also, at higher gas flow rates, number of small bubbles within the riser increases which leads to more collision and coalescence with large bubbles, resulting in longer length and higher velocities and frequencies due to larger buoyancy effects. However, large bubbles show larger lengths, velocities, and frequencies of appearance in the annulus riser compared to the circular riser. This can be attributed to the smaller flow area in the annulus riser and the higher gas velocity. In fact, smaller cross-sectional area makes longer bubbles under the same inlet gas flow rates, and this, in turn, brings about higher velocities and frequencies from large bubbles in the annulus riser. In the slug flow regime, Taylor bubbles and their behaviour are the main driving mechanism behind delivered liquid flow rate; essentially, longer Taylor bubbles with higher rising velocities lead to more liquid flow rate. As shown in Figs. 10a and 10 b, at low air flow rates (slug regime), Taylor bubbles of the annulus rise show slightly larger lengths with higher velocities; this can be probably the reason behind better performance (i.e., higher liquid flow rates) of annulus riser in slug flow regime.

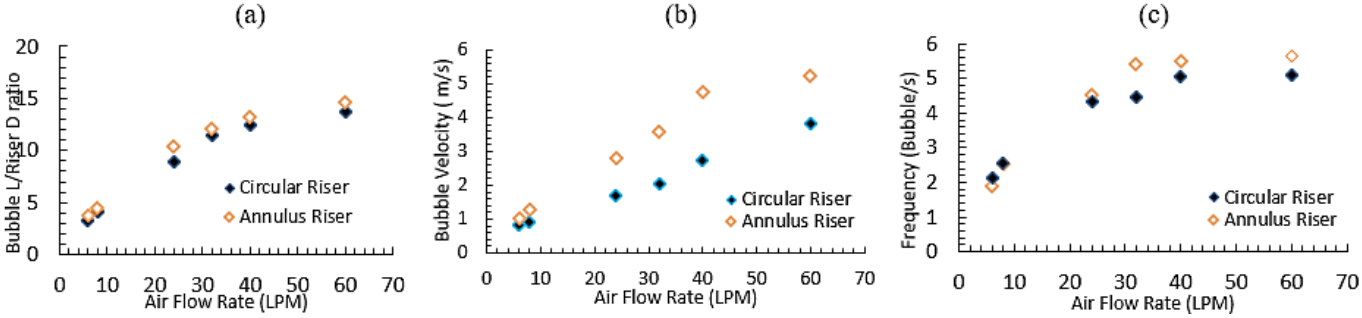

Fig. 10: Long bubbles (a) length over riser diameter, (b) velocity, and (c) frequency of appearance in the risers

4. Conclusions

In this study, the effect of an annulus riser pipe geometry on an airlift pump's performance was investigated. All experiments were conducted at a submergence ratio of 70% for both annulus and circular pump risers. The performance was mainly tested for 14 different input gas flowrates of 4-60 LPM. According to experimental observations and void fraction data, annulus geometry leads to higher void fraction and subsequently, faster slug-churn transition under the same inlet gas flow rate. Also, Taylor bubbles and long bubbles in churn pattern well as small bubbles and liquid phase in the liquid slug exhibit rotational movement around the inner rod while moving upward. In annulus geometry, Taylor bubbles were found to be longer with higher velocities and frequencies. The experimental results showed that mainly at lower inlet gas flow rates, the pump performed better with the annulus riser compared to that of the circular riser. However, at higher inlet gas flowrates, the circular riser produced better performance outcomes concluding that the circular riser is in fact the better choice for higher inlet gas flowrates. The pump's efficiency produced the same results when comparing the two setups as the lower inlet gas flowrates within the annulus riser produced a higher efficiency, and at higher inlet gas flowrates the pump was more

efficient in the circular riser. With the research results regarding lower gas inlet flowrates, further investigations regarding different submergence ratios, different tube diameters, or the influence of the annulus on mass transfer are highly suggested to further test the effects of the annulus. These findings help introduce airlift pumps to different industries and more remote locations where peak performance inlet gas supplies may be difficult.

Acknowledgements

The authors would like to acknowledge the support received from the Ontario Ministry of Agriculture and Rural Affairs (OMAFRA) Ontario Agri-Food Innovation Alliance Research Tier I Research Program (Grant 030647) to carry out the present research. The support of Natural Sciences and Engineering Research Council of Canada (NSERC) is also appreciated.

References

[1] W. H. Ahmed, A. M. Aman, H. M. Badr, and A. M. Al-Qutub, "Air injection methods: The key to a better performance of airlift pumps," *Exp. Therm. Fluid Sci.*, vol. 70, pp. 354–365, 2016, doi: 10.1016/j.expthermflusci.2015.09.022.

[2] S. Z. Kassab, H. A. Kandil, H. A. Warda, and W. H. Ahmed, "Air-lift pumps characteristics under two-phase flow conditions," *Int. J. Heat Fluid Flow*, vol. 30, no. 1, pp. 88–98, 2009, doi: 10.1016/j.ijheatfluidflow.2008.09.002.

[3] S. Z. Kassab, H. A. Kandil, H. A. Warda, and W. H. Ahmed, "Experimental and analytical investigations of airlift pumps operating in three-phase flow," *Chem. Eng. J.*, vol. 131, no. 1–3, pp. 273–281, 2007, doi: 10.1016/j.cej.2006.12.009.

[4] P. Hanafizadeh, S. Ghanbarzadeh, and M. H. Saidi, "Visual technique for detection of gas-liquid two-phase flow regime in the airlift pump," *J. Pet. Sci. Eng.*, vol. 75, no. 3–4, pp. 327–335, 2011, doi: 10.1016/j.petrol.2010.11.028.

[5] G. Ligus, D. Zajac, M. Masiukiewicz, and S. Anweiler, "A new method of selecting the airlift pump optimum efficiency at low submergence ratios with the use of image analysis," *Energies*, vol. 12, no. 4, 2019, doi: 10.3390/en12040735.

[6] C. T. Moisidis and E. G. Kastrinakis, "Two-phase flow pattern transitions of short airlift pumps," *J. Hydraul. Res.*, vol. 48, no. 5, pp. 680–685, 2010, doi: 10.1080/00221686.2010.515382.

[7] P. Hanafizadeh, M. H. Saidi, A. Karimi, and A. Zamiri, "Effect of bubble size and angle of tapering upriser pipe on the performance of airlift pumps," *Part. Sci. Technol.*, vol. 28, no. 4, pp. 332–347, 2010, doi: 10.1080/02726351.2010.496300.

[8] E. M. Fayyadh, N. M. Mahdi, and A. F. Mohammed, "The Effect of Air Injection System on Airlift Pump Performance," *FME Trans.*, vol. 48, no. 4, pp. 800–807, 2020, doi: 10.5937/fme2004800F.

[9] Z. neng Wang, Y. Kang, D. Li, X. chuan Wang, and D. Hu, "Investigating the hydrodynamics of airlift pumps by wavelet packet transform and the recurrence plot," *Exp. Therm. Fluid Sci.*, vol. 92, no. November 2017, pp. 56–68, 2018, doi: 10.1016/j.expthermflusci.2017.11.006.

[10] M. F. Khalil and H. Mansour, "Improvement of the performance of an air lift pump by means of surfactants," *Mansoura Eng. J*, vol. 15, no. 2, pp. 119–129, 1990.

[11] M. F. Khalil, K. A. Elshorbagy, S. Z. Kassab, and R. I. Fahmy, "Effect of air injection method on the performance of an air lift pump," *Int. J. Heat Fluid Flow*, vol. 20, no. 6, pp. 598–604, 1999, doi: 10.1016/S0142-727X(99)00051-X.

[12] R. Abed and W. H. Ahmed, "The effect of pulsating air injection on the development of two-phase flow instabilities in an airlift pump," *Exp. Therm. Fluid Sci.*, vol. 137, no. December 2021, p. 110678, 2022, doi: 10.1016/j.expthermflusci.2022.110678.

[13] P. Hanafizadeh, M. Moezzi, and M. H. Saidi, "Simulation of gas-liquid two phase flow in upriser pipe of gas-lift systems," *Energy Equip. Syst.*, vol. 2, no. 1, pp. 25–42, 2014, doi: 10.22059/ees.2014.5013.

[14] R. Abed, E. Chadwick, and W. H. Ahmed, "Two-phase flow behaviour in airlift pumps," *Int. Conf. Fluid Flow, Heat Mass Transf.*, no. 168, p. 168, 2018, doi: 10.11159/ffhmt18.168.

[15] Y. Qiang, W. Fan, C. Xiao, Y. Pan, and Y. Chen, "Effects of operating parameters and injection method on the performance of an artificial upwelling by using airlift pump," *Appl. Ocean Res.*, vol. 78, no. June, pp. 212–222, 2018, doi: 10.1016/j.apor.2018.06.006.

[16] F. S. Abou Taleb and J. A. Al-jarrah, "Experimental Study of an Air Lift Pump," *Eng. Technol. Appl. Sci. Res.*, vol. 7, no. 3, pp. 1676–1680, 2017, doi: 10.48084/etasr.1207.

[17] H. Tighzert, M. Brahimi, N. Kechroud, and F. Benabbas, "Effect of submergence ratio on the liquid phase velocity, efficiency and void fraction in an air-lift pump," *J. Pet. Sci. Eng.*, vol. 110, pp. 155–161, 2013, doi: 10.1016/j.petrol.2013.08.047.

[18] W. Fan, J. Chen, Y. Pan, H. Huang, C. T. Arthur Chen, and Y. Chen, "Experimental study on the performance of an air-lift pump for artificial upwelling," *Ocean Eng.*, vol. 59, pp. 47–57, 2013, doi: 10.1016/j.oceaneng.2012.11.014.
[19] D. J. Reinemann, "Theory of small-diameter airlift pumps," *Int. J. Multiph. Flow*, vol. 16, no. I, pp. 113–122, 1990, doi: https://doi.org/10.1016/0301-9322(90)90042-H.
[20] A. Kouremenos and J. Staios, "Performance of a small air-lift pump.," *Int. J. Heat Fluid Flow*, vol. 6, no. 3, pp. 217–222, 1985.
[21] S. H. Kim, C. H. Sohn, and J. Y. Hwang, "Effects of tube diameter and submergence ratio on bubble pattern and performance of air-lift pump," *Int. J. Multiph. Flow*, vol. 58, pp. 195–204, 2014, doi: 10.1016/j.ijmultiphaseflow.2013.09.007.
[22] A. A. Dare and O. Oturuhoyi, "Experimental Investigation of Air Lift Pump," *Engineering*, vol. 8, no. 1, pp. 56–62, 2007, [Online]. Available: https://www.ajol.info/index.php/ajst/article/view/155935
[23] C. H. Sohn, S. H. Kim, and J. Y. Hwang, "Effects of insertion of blunt body on bubble pattern and pumping performance in air-lift pump," *J. Mech. Sci. Technol.*, vol. 32, no. 2, pp. 969–976, 2018, doi: 10.1007/s12206-018-0147-8.
[24] R. Abed, M. M. Hussein, W. H. Ahmed, and S. Abdou, "Two-Phase Flow Mass Transfer Analysis of Airlift Pump for Aquaculture Applications," *Fluids*, vol. 6, no. 6, p. 226, 2021, doi: 10.3390/fluids6060226.